ELSEVIER

Journal of Photochemistry and Photobiology A: Chemistry 116 (1998) 69–73

Journal of Photochemistry and Photobiology A:Chemistry

Photoassisted dissolution of colloidal manganese dioxide in the presence of phenol

Ottó Horváth *, Katalin Strohmayer

Department of General and Inorganic Chemistry, University of Veszprém, P.O. Box 158, H-8201 Veszprém, Hungary

Received 10 March 1998; accepted 20 April 1998

Abstract

The UV–vis absorption spectrum of colloidal manganese dioxide in aqueous solution is considerably modified by addition of phenol. This is accounted for the formation of a charge-transfer complex on the surface of the MnO_2 particulates. Irradiation of this system in the range 310–590 nm leads to an enhanced reductive dissolution of the Mn(IV) species. The dependences of both the spectral change and the rate of the photoassisted dissolution on the phenol concentration show Langmuir-type functions, the evaluation of which gives the formation constant of the surface-located complex, $K = 1.3 \pm 0.3 \times 10^4\ M^{-1}$. The crucial role of this compound in the photoinduced reduction of manganese dioxide is also confirmed by the wavelength dependence of the quantum yield.

Keywords: Photoassisted dissolution; Colloidal manganese dioxide; Phenol

1. Introduction

Manganese is the eleventh most abundant element in the Earth's crust [1] and is an important micronutrient for all organisms [2]. It occurs in natural waters as insoluble Mn(III and IV) oxides and as soluble Mn^{2+} ions. Manganese(III, IV) oxide minerals are thermodynamically stable in oxygenated solutions and their formation in surface waters is a result of bacterial activity [3–8]. However, manganese oxide particles and crusts in natural waters can be reduced and dissolved by organic compounds with carboxyl, carbonyl, phenolic and alcoholic groups, increasing the mobility of manganese and its availability to organisms [9–11]. A significant steady-state concentration of soluble Mn(II) may be generated as a result of the localized action of reductants at the oxide surface in both fresh water and seawater [9,12]. Dissolution of manganese(III, IV) oxides by humic compounds, as well as by high molecular weight organics of similar structure indicated that this process may be an important degradative pathway for these organic compounds in some environments [13–15].

Experiments with both synthetic and natural Mn oxides showed that the enhanced dissolution rates in marine surface waters could be accounted for a marked stimulation of oxide reduction rates by sunlight [7,16,17]. Fulvic acids have been shown to dissolve manganese oxides via photocatalysed reaction [12,18]. The mechanism of photoreductive dissolution of Mn oxides is unknown, but it may include photochemical enhancement of ligand-to-metal charge transfer (LMCT) reactions between Mn oxides and adsorbed organic molecules [19]. In order to get more insight in this field, we have studied the photoassisted dissolution of MnO_2 in the presence of phenol. This model system has been chosen because MnO_2 is the predominant form of manganese oxides, and different phenolic compounds can also be found in surface waters. Phenol is an appropriate representative of them and is especially useful for photochemical study of the possible LMCT reaction because it does not absorb above 310 nm, preventing its direct excitation and inner-filter effect.

2. Experimental details

Analytical grade $KMnO_4$, $MnSO_4 \cdot 4H_2O$, sodium polyphosphate ($(NaPO_3)_6$), and phenol were used for the preparation of solutions studied. Triply distilled water served as solvent. A stock-solution of 4×10^{-4} M MnO_2 was prepared by the synproportional reaction of MnO_4^- and Mn^{2+} according to a modified version of the process described in the literature [20]. In order to approach the natural conditions, the MnO_2 stock-solution contained about 20% excess (i.e., 8×10^{-5} M) Mn^{2+} too. Thus, it was prepared by addition of 75 ml solution of 5.3×10^{-4} M $MnSO_4$ to 50 ml of 4×10^{-4}

---

* Corresponding author. E-mail: otto@vegic.sol.vein.hu

1010-6030/98/$ - see front matter
PII S1010-6030(98)00279-2

M $KMnO_4$. The reaction took place instantly, but MnO_2 was precipitated and settled down in a short time in the colloid solution. For this reason sodium polyphosphate was added to the $MnSO_4$ solution in the concentration of 4×10^{-4} M. This compound, as a polyelectrolyte, stabilized the produced colloid, so it did not change for weeks. However, at the same time, addition of polyphosphate significantly slowed down the synproportional reaction because its negatively charged surface repels MnO_4^- and bonds Mn^{2+}. Therefore, the complete conversion took several days. The reproducibility of the solution prepared by this method proved to be very good, indicating that the formed colloid MnO_2 particles were always of the same size and their distribution is probably monodisperse.

The absorption spectra were recorded on a GBC UV/VIS 911A spectrophotometer, using 1-cm quartz cuvettes. Typically the irradiations were carried out with 2.5 ml solutions in 1-cm cells at room temperature. During the photokinetic experiments solutions were homogenised by magnetic stirring. For continuous photolysis a 150-W medium pressure mercury arc lamp was applied with a cut-off filter to remove the radiation of $\lambda < 310$ nm. A 10-cm water filter was used to remove the infrared radiation. For quantum yield determination at different wavelengths an AMKO LTI system consisted of a 150-W high pressure Xe–Hg arc lamp and a monochromator were utilized. Incident light intensity was determined with a thermopile calibrated by ferrioxalate actinometry. Quantum yield measurements were carried out with samples of nearly 100% light absorption.

3. Results and discussion

3.1. Spectra and equilibrium

The absorption spectrum of the MnO_2 solution in the UV and visible range shows two broad overlapping bands with maxima at 225 and 388 nm (Fig. 1, curve *a*). In the concentration range examined ($0–4 \times 10^{-4}$ M) the Beer–Lambert's law is prevalid in this system, and for the peak of 388 nm 4680 ± 80 M^{-1} cm^{-1} was obtained as molar absorbance. Addition of 2×10^{-4} M phenol to this system modifies the spectrum to a certain extent (Fig. 1, curve *b*), but, concerning the concentration of MnO_2, it also follows the Beer–Lambert's law, with the molar absorbance of 5470 ± 90 M^{-1} cm^{-1} for the 395-nm peak.

Since the addition of phenol caused a perceptible change in the spectrum of MnO_2, the quantitative examination of the effect of phenol concentration was carried out. The absorbance increased in the range of 350–440 nm with the raising of the concentration of phenol (up to 10^{-4} M), and simultaneously the peak at 388 nm shifted to 395 nm (Fig. 2). At lower wavelengths the absorbance decreased, the band at 225 nm disappeared, and an isosbestic point arose at 351 nm, suggesting that MnO_2 existed in two states in the solution. Further increasing of phenol concentration caused smaller and smaller change in the absorbance at the peak. At the same time, an absorption peak at about 270 nm, due to the phenol in the bulk solution, appeared and increased linearly to the concentration of phenol (not shown). Both phenomena suggest that at lower concentrations ($< 10^{-4}$ M) the added phenol is mainly bound to the MnO_2 particulates, probably forming a surface-located complex. In the case of higher phenol concentrations, when most of the active (suitable for complex formation) places are occupied on the surface of the MnO_2 particulates, more and more phenol remains free in the bulk of the solution.

The plot of the absorbance at 395 nm vs. concentration of added phenol (Fig. 3) shows the characteristics of a Langmuir-type function. Although the precise nature of the interaction of phenol with manganese dioxide is not quite clear, it can be modelled as a complexation reaction on the surface sites of the MnO_2 particulates. Considering the formation of surface complexes as an equilibrium process, from the data

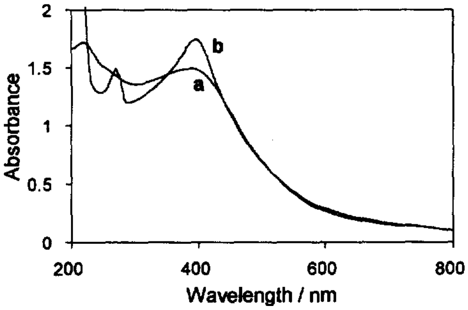

Fig. 1. Absorption spectrum of manganese-dioxide (3.2×10^{-4} M, with 6.4×10^{-5} M Mn^{2+}) in the absence (a) and in the presence (b) of phenol (2×10^{-4} M) ($\ell = 1$ cm).

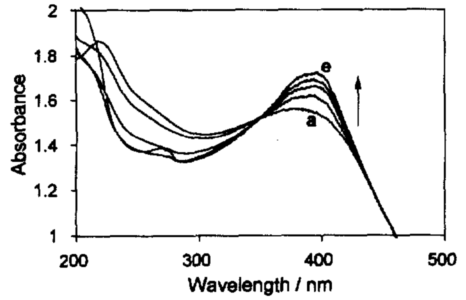

Fig. 2. Spectral effect of phenol addition to 3.2×10^{-4} M MnO_2. Concentrations of added phenol: 2×10^{-5}, 4×10^{-5}, 6×10^{-5} and 10^{-4} M.

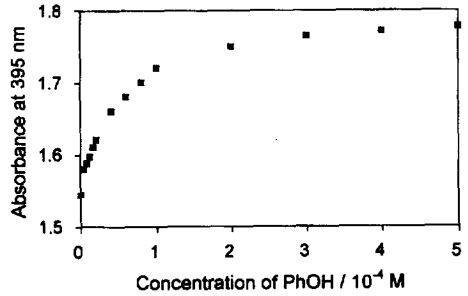

Fig. 3. Absorbance (at 395 nm) vs. C_{PhOH} plot ($\ell = 1$ cm, 3.2×10^{-4} M MnO_2).

of A_{395} vs. C_{PhOH}, the equilibrium constant of the following reaction can be determined:

$$\mathrm{MnO_2(F)+PhOH \Leftrightarrow MnO_2\text{–}PhOH = MnO_2(C)} \qquad (1)$$

'F' and 'C' in parentheses designate free and complexed metal centres, respectively, on the surface of the MnO_2 particulates. The equilibrium constant of the above reaction is

$$K=\frac{[\mathrm{MnO_2(C)}]}{[\mathrm{PhOH}][\mathrm{MnO_2(F)}]} \qquad (2)$$

The concentration of the active sites on the surface of particulates is much lower than the analytic concentration of Mn(IV) in this system. The following method, however, allows the determination of K regarding only the surface-sited Mn(VI) centres, no matter what their ratio to the total number of Mn(IV) centres is. Since in our system only MnO_2 absorbs light at 395 nm, its actual molar absorbance (ε) can be expressed in terms of molar absorbances regarding two cases: (1) when the system is phenol-free (ε_F), (2) when all metal-centres on the surface of particulates (i.e., all sites accessible to phenol) are complexed (ε_C):

$$\varepsilon=\alpha_F\varepsilon_F+\alpha_C\varepsilon_C \qquad (3)$$

where α_F and α_C are mole fractions of the free and complexed metal-centres. Eq. (3) can be formed to

$$\varepsilon=\frac{\varepsilon_F+\varepsilon_C K[\mathrm{PhOH}]}{1+K[\mathrm{PhOH}]} \qquad (4)$$

This equation can be rearranged to

$$\frac{\varepsilon-\varepsilon_F}{\varepsilon_C-\varepsilon}=K[\mathrm{PhOH}] \qquad (5)$$

The left side of this equation can also be expressed in terms of absorbances,

$$F=\left(\frac{A-A_F}{A_C-A}\right) \qquad (6)$$

where A_F is equal to the absorbance of the solution without phenol, while A_C represents the case of the total complexation of the surface sites. The latter one was estimated to be 1.81 (on the basis of Fig. 3). The plot of F vs. [PhOH] (Fig. 4) fits on a straight line running into the origin, and the slope of which is K. A fitting by the least-square method gave $1.51\pm0.05\times10^4\ \mathrm{M^{-1}}$ for the equilibrium constant. During this procedure the equilibrium concentration of the phenol ([PhOH]) was considered to be equal to the analytical concentration (C_{PhOH}), which was a rather strong approach, although it did not cause substantial error at the higher values of [PhOH]. Since the slope of the plot in Fig. 4 is basically determined by the points belonging to higher concentration values, the mentioned approach did not significantly influence the value of K determined. Of course, this equilibrium constant regards only the active sites on the surfaces of MnO_2 particulates, which are accessible to phenol. Eq. (4) can be formed to

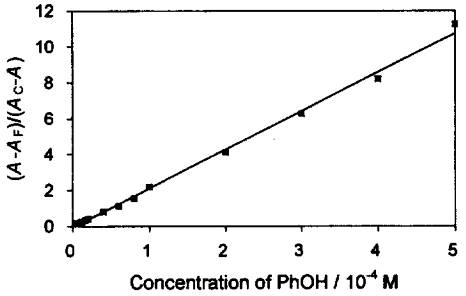

Fig. 4. Linearized representation of Fig. 3 for determination of the equilibrium constant.

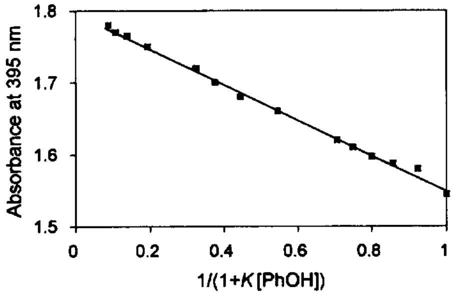

Fig. 5. Linearized representation of Fig. 3 for determination of ε_F and ε_C ($K=1.51\times10^4\ \mathrm{M^{-1}}$).

$$A=C\ell\varepsilon=C\ell\left(\varepsilon_C+\frac{\varepsilon_F-\varepsilon_C}{1+K[\mathrm{PhOH}]}\right) \qquad (7)$$

where C is the analytical concentration of MnO_2, ℓ is the path length of the cuvette. Plotting the values of absorbance A against $1/(1+K[\mathrm{PhOH}])$, the points must be placed along a straight line, the slope of which is $(\varepsilon_F-\varepsilon_C)C\ell$ (i.e., A_F-A_C), and its intercept is $\varepsilon_C C\ell$ (i.e., A_C). Fig. 5 shows that most of the points match conveniently the line (with equal scattering). Only few points, in the range $0.8<1/(1+K[\mathrm{PhOH}])<1.0$, deviate perceptibly, due to the approach ($C_{\mathrm{PhOH}}\cong[\mathrm{PhOH}]$) mentioned above. The good fitting confirms the reliability of the value of K defined above. The linear regression leads to the values of $4870\pm80\ \mathrm{M^{-1}\,cm^{-1}}$ and $5660\pm90\ \mathrm{M^{-1}\,cm^{-1}}$ for ε_F and ε_C, respectively, at 395 nm.

3.2. Photochemistry

Irradiation ($\lambda_{irr}>310$ nm) of the solution containing only MnO_2 (4×10^{-4} M) did not cause any permanent chemical change, not even after degassing. The spectral change (Fig. 6) of the solution containing 3.2×10^{-4} M MnO_2 and 2×10^{-4} M phenol suggests that in the photochemical reaction Mn(IV) is reduced, while phenol is oxidized. After 60–80 min of irradiation, practically the total amount of MnO_2 has been used up. The final product of reduction, on the basis of the change in the spectrum, may be Mn(II) or Mn(III) as well, because Mn(II) does not absorb at wavelengths higher than 200 nm, and Mn(III) shows absorption bands at 240 and 260 nm [21], which, however, overlap with the bands of phenol and its oxidation products. The initial slope of the

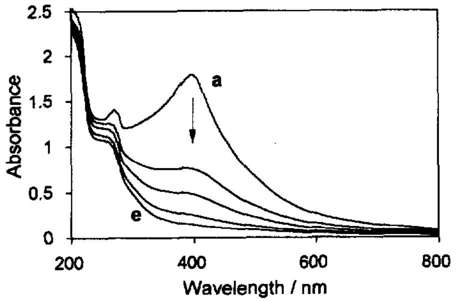

Fig. 6. Absorption spectra of 3.2×10^{-4} M MnO_2 with 2×10^{-4} M phenol after 0-, 10-, 20-, 40-, and 60-min irradiation ($\ell = 1$ cm).

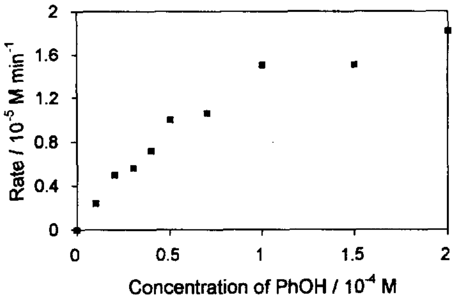

Fig. 7. Photochemical dissolution rate of MnO_2 as a function of the concentration of added phenol.

concentration vs. irradiation time plot was taken as the rate of the disappearance of MnO_2. Concentrations were calculated from the absorbances measured at 395 nm, knowing the actual molar absorbances. During the preliminary investigations it was proved that in the presence of phenol, the redox reaction also takes place in thermal way, though one order of magnitude slower. When the rate of photochemical reaction was determined, the overall rate of the MnO_2 disappearance was reduced by the thermal rate of reaction measured in the solution of the same composition (in dark).

Changing the concentration of phenol in the range 0–2 $\times10^{-4}$ M, the initial rate of reaction monotonously increased with C_{PhOH}, but its slope was more and more decreasing (Fig. 7). Since a similar, Langmuir-type curve was obtained for the function of A_{395} vs. C_{PhOH} (see Fig. 3), probably the rate of the photochemical reaction is directly proportional to the concentration of the surface-located charge-transfer complex formed between MnO_2 and phenol, i.e.,

$$dC/dt \sim [MnO_2(C)] \qquad (8)$$

The irradiated solutions absorbed the total amount of the incident light, thus the reaction rate is directly proportional to the mole fraction of the surface-complex. The proportional factor contains the intensity of the absorbed light (I_0), as well as the quantum yield of the redox reaction at the given wavelength or in the given range of wavelengths of irradiation (Φ), i.e.,

$$dC/dt = k\alpha_C;\ k \sim (I_0\Phi) \qquad (9)$$

Thus, according to the consideration above, the reaction rate vs. mole fraction (i.e., $K[PhOH]/(1+K[PhOH])$) plot should be linear. Using $K = 1.51\times10^4\ M^{-1}$ for the calculation of the actual mole fractions, our data points were placed indeed along a straight line with approximately equal scattering (not shown). However, searching for the value of K giving the best fit of this linear regression, we could determine the formation constant of the surface-located complex by an independent, photochemical method ($K = 1.10\times10^4\ M^{-1}$). Using this value, Fig. 8 demonstrates the really good fit of our data. This value of K is in good agreement with that obtained by spectrophotometric method ($1.5\times10^4\ M^{-1}$), and the average of them ($K = 1.3\pm0.3\times10^4\ M^{-1}$) can be accepted as a final result. The accordance of the spectral and photochemical results suggests that only those Mn(IV) centres are photoactive to which phenol is bound. Similarly, formation of surface bound complexes was found to play a significant role in the photoreductive dissolution of different colloidal metal oxides in the presence of various organic compounds [19,22–24].

In the case of constant phenol concentration (2×10^{-4} M), no significant change was experienced in the reaction rate by changing the concentration of MnO_2 in the range 8×10^{-5}–3.2×10^{-4} M (assuring the total absorption of light by using cuvettes of appropriate path length). This fact confirms the conclusion that the mole fraction of the surface-located charge-transfer complex is a determinant factor in the studied photoinduced redox reaction because it remains unaltered in the case of constant phenol concentration.

For the characterization of a photoactive species, its action spectrum, i.e., the dependence of the quantum yield of the reaction on the wavelength of irradiation may serve with important pieces of information. The results obtained for the

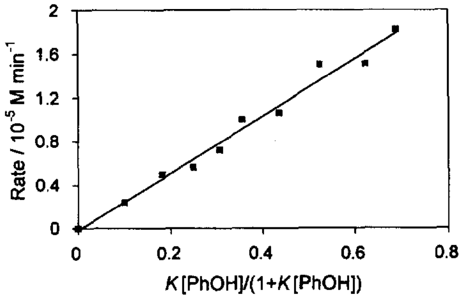

Fig. 8. Photochemical dissolution rate of MnO_2 as a function of the mole fraction of the surface-localized charge-transfer complex (between MnO_2 and phenol, $C_{MnO_2} = 3.2\times10^{-4}$ M, $K = 1.10\times10^4\ M^{-1}$).

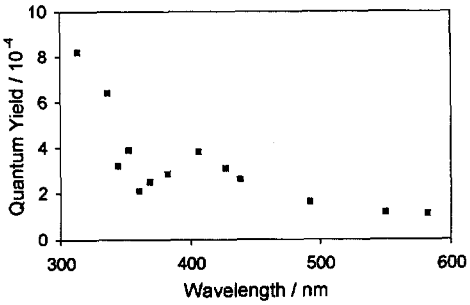

Fig. 9. Action spectrum of MnO_2 in the presence of 1.5×10^{-4} M phenol, ($C_{MnO_2} = 3.2\times10^{-4}$ M).

reaction studied in the range of 310–590 nm showed that the action spectrum (in the presence of 1.5×10^{-4} M phenol, Fig. 9) is in close correlation with the absorption spectrum of MnO_2 (see Fig. 1). The modification in the spectrum caused by the addition of phenol is not drastic, partly because only a smaller fraction of Mn(IV) centres are accessible to phenol. (i.e., the surface sites). Thus, the larger fraction of light absorbed by the system excited MnO_2 units not bound to phenol. Since only complexed Mn(IV) centres are redox-active, the photoinduced reaction may operate with two different mechanisms. In one of them, only the direct excitation of the surface-located complex can lead to ligand-to-metal charge-transfer reaction, while in the other one, the excitation of a MnO_2 unit not bound to phenol may also be effective due to an energy transfer from the excited MnO_2 unit to a surface-complex. The probability of the latter process may also be directly proportional to the mole fraction of the surface-complex, thus, none of these mechanisms can be precluded on the basis of our present results. The separation of these possibilities needs further investigations.

4. Conclusions

Analysis of the UV–visible absorption spectrum of colloidal manganese dioxide in the presence of phenol clearly indicated the formation of a complex between the Mn(IV) centres on the surface sites of particulates and the organic compound added. The rate of the photoinduced reductive dissolution of MnO_2 in this system proved to be proportional to the mole fraction of the surface-located complex and offered an independent method for the determination of the complex formation constant. The accordance of the spectral and photochemical results unambiguously showed that the key step of the dissolution is a ligand-to-metal charge transfer process involving this complex. Elucidation of the mechanism, taking both direct excitation and energy transfer into account, needs further studies.

Acknowledgements

Support of this work by the Hungarian National Science Foundation (OTKA, project number T016322) is gratefully acknowledged. O.H. is indebted to the Alexander von Humboldt Foundation for the donation of the AMKO LTI photolysis system used in this study.

References

[1] G.P. Glasby, Oceanogr. Mar. Biol. Annu. Rev. 22 (1994) 169.
[2] W. Kaim, B. Schwederski, Bioanorganische Chemie, B.G. Teubner, Stuttgart, 1991, pp. 72–86.
[3] S. Emerson, S. Kalhorn, L. Jacobs, B.M. Tebo, K.H. Nealson, R.A. Rosson, Geochim. Cosmochim. Acta 46 (1982) 1073.
[4] B.M. Tebo, K.H. Nealson, S. Emerson, L. Jacobs, Limnol. Oceanogr. 29 (1984) 1247.
[5] B.M. Tebo, S. Emerson, Appl. Environ. Microbiol. 50 (1985) 1268.
[6] W.G. Sunda, S.A. Huntsman, Limnol. Oceanogr. 32 (1987) 552.
[7] W.G. Sunda, S.A. Huntsman, Deep Sea Res. 35 (1988) 1297.
[8] W.G. Sunda, S.A. Hunstman, Limnol. Oceanogr. 35 (1990) 325.
[9] A.T. Stone, J.J. Morgan, Environ. Sci. Technol. 18 (1984) 450.
[10] A.T. Stone, J.J. Morgan, Environ. Sci. Technol. 18 (1984) 617.
[11] A.T. Stone, Geochim. Cosmochim. Acta 51 (1987) 919.
[12] W.G. Sunda, S.A. Hunstman, G.R. Harvey, Nature 234 (1983) 301.
[13] W.E. Baker, Geochim. Cosmochim. Acta 37 (1973) 269.
[14] R.E. Guy, C.L. Chakrabarti, Can. J. Chem. 54 (1976) 2600.
[15] W.G. Sunda, D.J. Kieber, Nature 367 (1994) 62.
[16] W.G. Sunda, S.A. Huntsman, Limnol. Oceanogr. 28 (1983) 924.
[17] W.G. Sunda, S.A. Huntsman, Mar. Chem. 46 (1994) 133.
[18] T.D. Waite, R. Szymczak, in: G.R. Helz, R.G. Zepp, D.G. Crosby (Eds.), Aquatic and Surface Photochemistry, Lewis, Boca Raton, 1994, pp. 39–52.
[19] T.D. Waite, I.C. Wrigley, R. Szymczak, Environ. Sci. Technol. 22 (1988) 778.
[20] C. Lume-Pereira, S. Baral, A. Henglein, E. Janata, J. Phys. Chem. 89 (1985) 5572.
[21] G.L. Donald, C.R. Moylan, T. Hayashi, J.I. Brauman, J. Am. Chem. Soc. 109 (1987) 3003.
[22] T. David Waite, F.M.M. Morel, J. Coll. Interface Sci. 1 (1984) 102.
[23] B. Sulzberger, H. Laubscher, G. Karametaxas, in: G.R. Helz, R.G. Zepp, D.G. Crosby (Eds.), Aquatic and Surface Photochemistry, Lewis, Boca Raton, 1994, pp. 53–73.
[24] L.A.G. Rodenas, A.M. Iglesias, A.D. Weisz, P.J. Morando, M.A. Blesa, Inorg. Chem. 36 (1997) 6423.